Clinical Chemistry 60:6
864–872 (2014)

Genotyping Accuracy of High-Resolution DNA Melting Instruments

Mei Li,[1,2] Luming Zhou,[1] Robert A. Palais,[3] and Carl T. Wittwer[1*]

BACKGROUND: High-resolution DNA melting is a closed-tube method for genotyping and variant scanning that depends on the thermal stability of PCR-generated products. Instruments vary in thermal precision, sample format, melting rates, acquisition, and software. Instrument genotyping accuracy has not been assessed.

METHODS: Each genotype of the single nucleotide variant (SNV) (c.3405–29A>T) of *CPS1* (carbamoyl-phosphate synthase 1, mitochondrial) was amplified by PCR in the presence of LCGreen Plus with 4 PCR product lengths. After blinding and genotype randomization, samples were melted in 10 instrument configurations under conditions recommended by the manufacturer. For each configuration and PCR product length, we analyzed 32–96 samples (depending on batch size) with both commercial and custom software. We assessed the accuracy of heterozygote detection and homozygote differentiation of a difficult, nearest-neighbor symmetric, class 4 variant with predicted ΔT_m of 0.00 °C.

RESULTS: Overall, the heterozygote accuracy was 99.7% (n = 2141), whereas homozygote accuracy was 70.3% (n = 4441). Instruments with single sample detection as opposed to full-plate imaging better distinguished homozygotes (78.1% and 61.8%, respectively, χ^2 $P < 0.0005$). Custom software improved accuracy over commercial software ($P < 0.002$), although melting protocols recommended by manufacturers were better than a constant ramp rate of 0.1 °C with an oil overlay. PCR products of 51, 100, 272, and 547 bp had accuracies of 72.3%, 83.1%, 59.8%, and 65.9%, respectively ($P < 0.0005$).

CONCLUSIONS: High-resolution melting detects heterozygotes with excellent accuracy, but homozygote accuracy is dependent on detection mode, analysis software, and PCR product size, as well as melting temperature differences between, and variation within, homozygotes.

High-resolution DNA melting is a simple method of genotyping that uses dyes instead of probes. PCR products are directly melted without additional processing. Advantages include low contamination risk, high speed, and high analytical sensitivity *(1–4)*. High-resolution melting is widely used in research and clinical diagnostics for detecting DNA sequence variants, either known (genotyping) or unknown (scanning). Most single nucleotide variants (SNVs),[4] as well as most small deletions or insertions, are easily genotyped, often resulting in reduced costs and sequencing burden for many analyses *(5–9)*. Heterozygotes introduce large shape changes in the melting curves and are easy to detect, with accuracies approaching 100% *(10)*.

In contrast to heterozygous variants, detecting homozygous variants typically depends on melting temperature (T_m) shifts and usually requires high-resolution melting. Class 1 and 2 SNVs exchange A:T and G:C base pairs with a T_m difference (ΔT_m) of about 1 °C in small PCR products *(2)*. These constitute about 84% of human SNVs and are easily detected on high-resolution melting instruments. However, about 16% of SNVs (class 3 and 4) simply switch bases while retaining the same base pair, having predicted ΔT_m values of 0.0–0.4 °C between homozygotes. About one quarter of class 3 and 4 SNVs (4% overall) are "nearest neighbor symmetric" or "base-pair neutral" homozygotes with predicted ΔT_m values of 0.0 °C *(2, 11)*. These SNVs and some small insertions or deletions with ΔT_m values close to 0.0 °C are the most difficult to differentiate by melting analysis *(12)*. Even with predicted ΔT_m values near or at zero, some of these can be resolved by high-resolution melting, possibly because

[1] Department of Pathology, University of Utah Medical School, Salt Lake City, UT; [2] current address: Laboratory Center, the Second Hospital of Dalian Medical University, Dalian, China; [3] Department of Mathematics, Utah Valley University, Orem, UT.
* Address correspondence to this author at: Department of Pathology, University of Utah Medical School, 50 N Medical Drive, Salt Lake City, UT 84132. Fax 801-581-6001; e-mail carl.wittwer@path.utah.edu.

Received December 6, 2013; accepted March 25, 2014.
Previously published online at DOI: 10.1373/clinchem.2013.220160

[4] Nonstandard abbreviations: SNV, single nucleotide variant; T_m, melting temperature; LS96, LightScanner 96; Rotor36/72, RotorGene Q (Rotor36, RotorGene Q with a 36-tube rotor; Rotor72, RotorGene Q with a 72-tube rotor); LC480, LightCycler 480; Piko, PikoReal 96.

of stability effects that go beyond the nearest neighbor theory *(13)*.

The genotyping accuracy of high-resolution melting instruments has not been directly assessed. In prior studies, the precision of early instruments was measured by the SD of the T_m (T_mSD) of multiple identical samples *(14–16)*. At that time, there were large differences among melting instruments, including sample format, melting rates, data density, and acquisition mode. Today, many differences remain, new instruments have been introduced, and it is not clear which of the many factors determine genotyping accuracy.

Our goal was to establish the genotyping accuracy of instruments that claim to perform high-resolution DNA melting by use of a range of PCR product lengths. Anticipating excellent results for heterozygotes on all instruments, we focused on differentiating homozygotes by using a difficult class 4 SNV from human genomic DNA with a predicted ΔT_m of 0.0 °C. We also sought to find the instrument and assay characteristics that contribute to genotyping accuracy.

Materials and Methods

GENERATION OF PCR PRODUCTS

Four PCR products of different lengths (51, 100, 272, and 547 bp) covering the same SNV in human genomic DNA [rs3213784, c.3405–29A>T in *CPS1* (carbamoyl-phosphate synthase 1, mitochondrial)] were amplified by nested PCR. To create the outer PCR products of 691 bp, human DNA of each genotype (A/A, A/T, and T/T) was amplified from *CPS1* with primers GAAATCAGGTTCTGGGCTGA and TTC CTCTTTTTCCACCAACC. Amplification was performed in 10-μL volumes with 50 ng genomic DNA, 200 μmol/L each deoxynucleotide triphosphate, 0.4 U KlenTaq™ (AB Peptides), 88 ng TaqStart antibody (Clontech), 2 mmol/L $MgCl_2$, 50 mmol/L Tris (pH 8.3), 500 μg/mL BSA, 0.5 μmol/L primers, and 1× LCGreen® Plus dye (BioFire Diagnostics) with a 25-μL mineral oil (Sigma-Aldrich) overlay. We used a CFX96™ (Bio-Rad) instrument with an initial denaturation at 95 °C for 2 min, followed by 25 cycles of 95 °C for 20 s, 65 °C for 20 s, and 72 °C for 30 s and cooling to 15 °C. The 3 genotypes (A/A, T/T, and A/T) were confirmed by sequencing.

Each PCR product length and genotype was amplified in 96-well plates in 50-μL volumes with a 40-μL overlay on either PTC200 (Bio-Rad) or CFX96 instruments. The reactions included 2 μL of a 10 000-fold dilution of the 691-bp PCR product. Other PCR components were the same as those used to amplify the 691-bp template. Primers for 51-, 100-, 272-, and 547-bp inner products were: AGTCAAGTCTAG TATTAGCATAAACCT and AAGGAAGGGGAAA AAAAGCAG; ATAGGTTGTCTGGAACTGTTCTG and TCATAGCAGACCCACTGGAA; TTGGTTGAT TGTCCTGGTGA and CAGTCACTACAAAGAAAT TGGACA; and CAGAAAGGGCAAACTTTGGA and GGAGACTAGAGGGTAGAAGAGGAAA, respectively. PCR was performed with an initial denaturation at 95 °C for 2 min, followed by 25 cycles of 95 °C for 15 s, annealing at 65 °C (15 s for 51 and 100 bp; 20 s for 272 and 547 bp), and extension at 72 °C (10 s for 51 bp; 15 s for 100 bp; 20 s for 272 bp; 30 s for 547 bp), then 95 °C with a 20-s hold, and cooled to 15 °C. We pooled PCR products by genotype for each product length. The mineral oil was discarded after centrifugation (1500*g* for 5 min). All PCR products were scanned on a LightScanner® 96 (BioFire Diagnostics) (LS96) to confirm the genotypes. We used nested PCR products as template instead of genomic DNA because the intent was to isolate and test the melting function of each instrument.

INSTRUMENTS AND TEMPERATURE VERIFICATION

We used 9 high-resolution melting instruments with excitation and emission wavelengths compatible with LCGreen Plus for comparison: HR-1™ (BioFire Diagnostics), LightScanner® 32 (BioFire Diagnostics) (LS32), LS96, Rotor-Gene® Q (36 and 72 sample carousels, Qiagen) (Rotor36/72), LightCycler® 480 (Roche) (LC480), CFX96, StepOnePlus™ (Thermo Fisher Scientific), Eco™ (Illumina), and PikoReal™ 96 (Thermo Fisher Scientific) (Piko). The instrument characteristics are listed in Supplemental Table 1, which accompanies the online version of this article at http://www.clinchem.org/content/vol60/issue6.

The sample temperatures of all instruments except for the Rotor36/72 were monitored with a J-type microthermocouple (5SRTC; Omega) and conditioned (USB-TC01; National Instruments) to calculate the ramp rate during melting. The sample temperatures of Rotor36/72 were measured with the temperature-sensitive sulforhodamine B dye, and the ramp rate was calculated by correlating fluorescence to temperature *(17)*.

MELTING ACQUISITION

We randomized 32–96 samples of 3 genotypes into capillaries, tubes, or plates, ranging from 10 to 20 μL, depending on the batch size and sample volumes recommended by the manufacturers. Four runs, 1 for each product size, were melted in each instrument along with 3 known genotype standards. We used both the 36 and 72 rotors on the RotorGene, for 10 instrument configurations. The 4 PCR products were melted from 65 to 92 °C in all instruments under high-resolution melting conditions as recommended by the manufacturers.

Melting was also performed at a common rate (0.1 °C/s) with a 10-μL oil overlay *(17)* on the LC480,

Table 1. Recommended and measured melting rates on high-resolution melting Instruments.

Instrument	Recommended instrument setting	Measured ramp rate (°C/s)[a]	Turnaround time (min)	Batch size	Throughput (samples/h)
HR-1	0.3 °C/s	0.3	1.5	1	40
LS32	0.3 °C/s	0.3	2.5	32	24
LS96	0.1 °C/s	0.1	5	96	1152
Eco	0.1 °C/s	0.08	7	48	411
LC480	25 acquisitions/°C	0.04	9	96	640
Piko	step (0.04 °C)/hold (1 s)	0.01	40	96	144
Rotor36/72	ramp (0.1 °C)/hold (2 s)	0.01	40	36/72	54/108
CFX96	step (0.2 °C)/hold (10 s)	0.01	50	96	115
StepOnePlus	0.3% ramp	0.005	95	96	61

[a] Measured with a microthermocouple or by temperature-sensitive fluorescence [Sanford and Wittwer *(17)*].

CFX96, Rotor36/72, and Piko. Because ramp rates cannot be programmed directly in these instruments, we adjusted instrument settings (acquisitions/°C, step, ramp, and/or hold) empirically to obtain 0.1 °C/s with a thermocouple or fluorescence.

HIGH-RESOLUTION MELTING ANALYSIS

The data obtained with the manufacturers' recommended melting conditions were analyzed on custom software written in LabView *(1, 18, 19)*. We used analysis with common software to focus on differences between instrument platforms, not software. The custom software sequentially processes melting data in 3 steps as previously detailed *(1)*. First, data is normalized between 0% and 100% fluorescence, including exponential background subtraction *(19)*, so that the pre- and post- melting regions are horizontal, relate to DNA helicity, and can be compared to predicted curves generated by uMelt *(20)* (https://www.dna.utah.edu/umelt/umelt.html). Second, and at user discretion, curves are overlaid at low fluorescence (high temperature) by shifting curves along the temperature axis until they are superimposed to focus on curve shape, not T_m. Finally, curves are displayed as difference plots that display all curves as the difference from wild-type curves. The custom software is available for noncommercial use by request from 1 of the authors (R.A. Palais).

The custom software best detects heterozygotes by shape changes of normalized and overlaid melting curves displayed on difference plots. Homozygotes are detected on difference plots with or without overlay and the use of A/A and T/T standards. Overlay of melting curves (also known as temperature shifting) is used when it helps to distinguish genotypes. In this study, overlay was particularly useful in analyzing homozygotes on some instruments with full-plate imaging. Regardless, all samples were analyzed both with and without curve overlay. All data were genotyped to determine: (*a*) the accuracy of heterozygous calls, (*b*) the accuracy of calling A/A vs T/T homozygotes, and (*c*) the analytical sensitivities of A/A and T/T calls. The T_m was taken as the peak temperature on negative derivative plots. For the 2-domain, 547-bp product, the T_m of the larger (higher-temperature) transition was used.

In some studies, we compared the instrument's own commercial software to the custom, common software. Commercial software results were obtained by manual inspection, autoclustering, or instrument genotyping as available from the different manufacturers.

Linear regression, χ^2, and *t*-test analysis were performed with SPSS 21 (IBM).

Results

Many parameters can affect the accuracy of genotyping by high-resolution melting. For example, different manufacturers recommend widely different melting rates for fluorescent high-resolution DNA melting. The instruments we studied here vary over a 60-fold range from 0.005 to 0.3 °C/s, resulting in turnaround times of 1.5 to 95 min (Table 1). Instead of the direct and simple °C/s as the unit of melting rate, various manufacturers have adopted creative but confusing units, such as, "X acquisitions/°C," "X°C step with a Y s hold," "X°C ramp with a Y s hold," or "X% ramp." Empirical measurement is necessary to convert these units to °C/s. Additional differences between instruments include container format (capillaries, plates, and tubes), sample volumes, number of tubes or wells, excitation and emission wavelengths, detection mode (full-plate imaging vs single sample interrogation), detector type, continuous or step acquisition, and analy-

sis software (see online Supplemental Table 1). Combining these instrument differences (that may all affect melting curve precision) with assay differences (ΔT_m, PCR product size, SNV class, PCR master mix, and dyes) makes determining the most relevant parameters a daunting task. Therefore, we limited our study to comparing instruments and PCR product sizes surrounding a single SNV using a single master mix and dye. Certain parameters, such as melting rate and dye comparisons, will best be done on single instruments and are left for future studies.

Representative melting curves of the 3 different genotypes (A/A, A/T, T/T) within 4 different PCR product lengths are shown in Fig. 1. PCR products <300 bp appear to melt in a single domain, whereas the larger 547-bp product melts in 2 domains. Heterozygotes are usually easy to distinguish from homozygotes, although the area between the curves becomes smaller as the product size increases.

The overall analytical sensitivity of heterozygotes was 99.7% (2135/2141) including all 10 instrument configurations, 2 melting conditions (manufacturer recommended and 0.1 °C/s with oil), and 2 software analyses (original manufacturer and custom software). The analytical specificity was 100%. False negatives occurred only in the 547-bp product. With manufacturer-recommended melting conditions and software, 5 heterozygous variants were misjudged as homozygotes, including 1 sample classified as A/A on the LC480 (97%) and 4 as T/T on StepOnePlus (87%). With a ramp rate of 0.1 °C/s, oil, and custom analysis, 1 heterozygote was misjudged as A/A on the Rotor72 (96%). Under manufacturers' melting conditions and custom software, 100% heterozygote accuracy was obtained on all instruments and product sizes.

In contrast to heterozygote detection, the 2 different homozygotes were very hard to distinguish from each other, as expected by their predicted ΔT_m of 0.0 °C *(2, 13)*. Genotyping accuracy varied with the instrument and with PCR product size. Overall, only 3121 of 4441 homozygotes (70.3%) were correctly genotyped.

The effect of curve overlay on genotyping homozygotes on instruments with full-plate imaging is shown in Fig. 2. On some instruments, curve overlay clearly enabled homozygous genotyping, whereas without overlay, temperature gradients across the plate could mask genotype shape differences. However, this advantage of curve overlay was instrument dependent; on another 96-well instrument with full-plate imaging, overlay had little effect, i.e., overlay could reveal genotype patterns only if the underlying precision of the curve shape was high enough.

With all relevant data considered, instrument factors that were highly significant included the melting

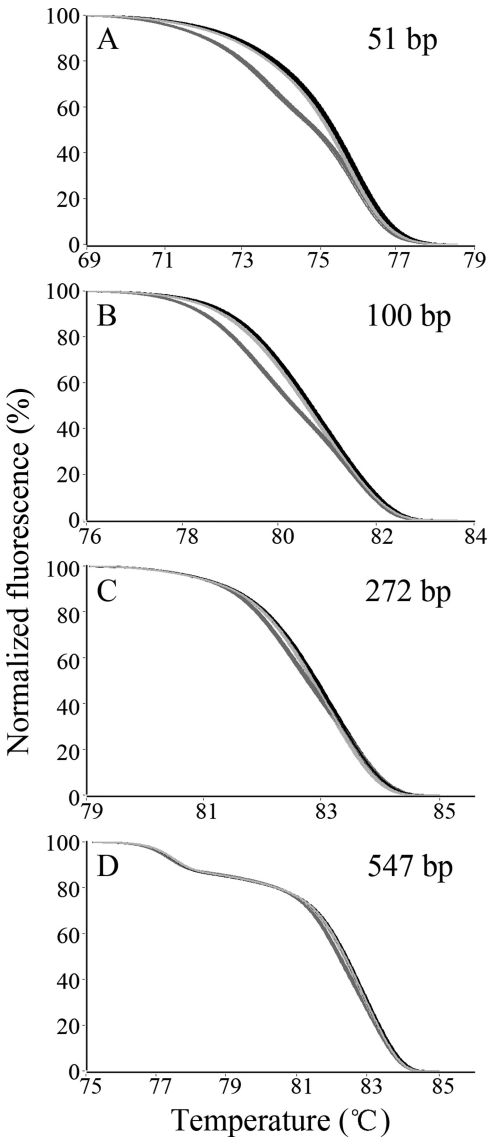

Fig. 1. Normalized melting curves of the 3 SNV genotypes within 4 PCR products of different sizes [(A), 51 bp; (B), 100 bp; (C), 272 bp; and (D), 547 bp].

The black, light gray, and dark gray curves indicate the wild-type, homozygous, and heterozygous genotypes, respectively, without overlay. In all cases, the heterozygotes are easy to distinguish from the homozygotes, but the wild-type and homozygous genotypes are difficult to differentiate. Single melting domains are present in the first 3 PCR products, but 2 are present in the longest product. Each panel shows 32 samples of random genotype obtained on the HR-1 at 0.3 °C/s.

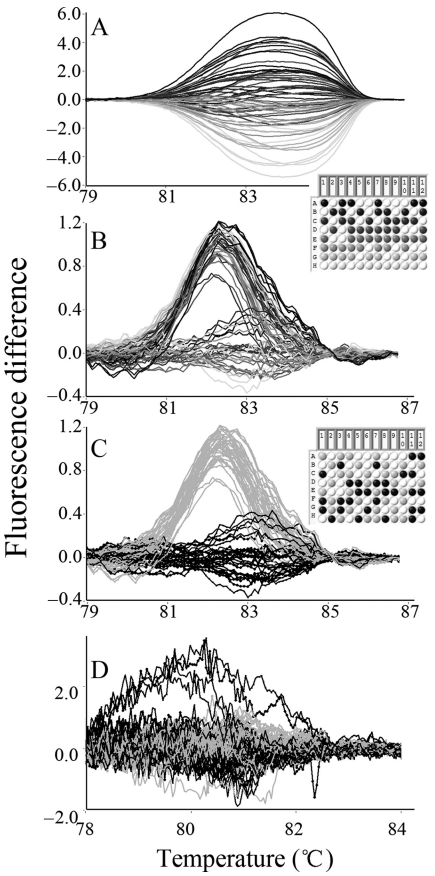

Fig. 2. Effect of curve overlay on homozygote differentiation.

Wild-type and homozygous genotypes are not separated on some instruments with full-plate imaging unless curve overlay is applied. The inset between panels (A) and (B) shows the heterozygote wells in white with the homozygotes as different shades of gray. The gray level correlates to different rows of a 96-well plate, not the homozygous genotypes. (A), Without curve overlay, the spread observed on difference plots correlates to plate position, not genotype. That is, a preponderance of lighter lines lower in the graph indicates that the difference plot is dominated by temperature differences across plate columns. (B), After curve overlay, the difference plots split into 2 clear genotype clusters that both include all different shades of gray (plate positions), indicating that the overlay has removed the temperature gradient effect to allow definitive genotyping. (C), The plate wells are now shaded by genotype (black = AA, gray = TT), showing the clear separation between homozygous genotypes on the difference plot. (D), On some full-plate imaging instruments, the homozygous genotypes are not separated, even after overlay. Wild-type and homozygous variant data shown in (A) through (C) were obtained on a LS96 at 0.1 °C/s, and (D) was from a Piko at 0.01 °C/s. All panels show difference plots of the 100-bp PCR product.

protocol, detection mode, and software (Table 2). Melting protocols were more accurate when performed as described by the manufacturer, rather than at 0.1 °C with an oil overlay ($P < 0.0005$). Single sample detection was more accurate than full-plate imaging ($P < 0.0005$). Those instruments that interrogate samples individually did better as a group than those with full-plate illumination and acquisition. Finally, the custom software genotyped more accurately than the various commercial software packages provided with the instruments ($P = 0.002$). Although no monotonic trend was apparent, the 51-, 100-, 272-, and 547-bp products had accuracies of 72.3%, 83.1%, 59.8%, and 65.9%, respectively ($P < 0.0005$).

Instrument and PCR product size effects are individually evaluated in Fig. 3, Fig. 4, online Supplemental Fig. 1, and online Supplemental Table 2. Online Supplemental Table 2 compares the homozygous genotyping accuracy for specific instruments and PCR product sizes, analyzed by both commercial and custom software. Custom software improved accuracies on the LS32, LS96, and LC480 for multiple size products. In only 1 instance (100-bp product on the StepOnePlus) was the commercial software significantly better than the custom software. Further instrument and size comparisons used only the custom software.

The analytical sensitivities of correctly detecting A/A and T/T homozygotes are shown in Fig. 3, separating each genotype along 1 dimension. All 10 different instrument configurations are plotted, and 1 panel is provided for each PCR product length. Any biases for incorrect A/A or T/T calls are reflected by the instrument position in each graph (upper left vs lower right).

Overall homozygote accuracies by instrument and PCR product size are shown in Fig. 4 and online Supplemental Table 2. In Fig. 4, the instruments are ordered according to decreasing recommended melting rates. Contrary to expectation, accuracy did not appear to improve with slower melting rates. Indeed, there was a trend toward better accuracy with faster rates. When the log of the melting rate was plotted against accuracy similar to Fig. 4, the correlation of rate to accuracy was slightly positive (linear regression $r = 0.3$, $P = 0.057$, data not shown).

Of the homozygotes, the 100-bp product was the easiest to genotype, with 100% accuracy in 7 of the 10 instrument configurations. The 272-bp product was the most difficult to genotype, and no instrument achieved 100% accuracy. Some instruments were consistently good across all product sizes (HR-1 and CFX96). Others were excellent with short products, but not with long products (Rotor36 and 72). Variation in the genotyping accuracy of the different rotor sizes of the same instrument may result from (*a*) different recommended sample volumes for each carousel, (*b*) total

Table 2. Characteristics that affect the ability to distinguish homozygotes.

Characteristic and classification	n	Accuracy (%)	P[a]
Instrument factors			
Melting protocol[b]			**<0.0005**
Recommended by manufacturer	1004	72.7	
Ramp rate 0.1°C/s, oil overlay	1038	62.9	
Detection mode			**<0.0005**
Single sample detection	2268	78.1	
Full-plate imaging	2173	61.8	
Acquisition mode			0.114
Continuous	1631	68.9	
Step	2810	71.1	
Software[c]			**0.002**
Custom	1709	74.4	
Commercial	1618	69.5	
Assay factors			
Amplicon size			**<0.0005**
51 and 100 bp	2222	77.7	
272 and 547 bp	2219	62.8	
ΔT_m[d]			
Single sample detection			**<0.0005**
$P < 0.05$	611	88.4	
$P \geq 0.05$	297	64.0	
Full-plate imaging			0.12
$P < 0.05$	222	65.8	
$P \geq 0.05$	655	71.3	
T_mSD (°C)			**0.010**
Single sample detection	24	0.058 (0.067)[e]	
Full-plate imaging	16	0.112 (0.056)[e]	

[a] All characteristics evaluated by χ^2 analysis (except *t*-test for T_mSD. *P* values < 0.05 are shown in bold.
[b] Two melting protocols were compared on 5 instruments for each product size.
[c] Commercial software provided by each instrument was compared to custom software [Gundry et al. *(18)*, Palais and Wittwer *(19)*] modified to accept input from all instruments. All 10 instrument configurations and all 4 product sizes were analyzed by both manufacturer and custom software, except for the HR-1 (instrument and custom software are the same) and samples melted at 0.1 °C/s (custom software only).
[d] T_m difference between A/A and T/T obtained from the temperature peaks on negative derivative curves using custom software.
[e] Values [mean (SD)] are of T_mSD, not accuracy.

volume load per carousel, and (*c*) different fluid (air) dynamics between 36- and 72-tube carousels.

Assay characteristics also contributed to homozygote genotyping success. Genotyping accuracy was better in smaller products than in larger products ($P < 0.0005$), although the relationship was not monotonic. The ΔT_m between homozygotes predicts better genotyping success in instruments with single sample detection ($P < 0.0005$), but not full-plate imaging ($P = 0.12$). Furthermore, the T_mSD is lower in instruments with single sample detection than those with full-plate imaging ($P = 0.01$). The smaller the T_mSD of an instrument, the greater the expected accuracy of genotyping, as previously described *(16)*. For any given SNV, the probability of distinguishing homozygotes increases as ΔT_m increases. Attempts to combine ΔT_m and T_mSD as a predictor of accuracy were not very successful, giving an R^2 of only 0.256, $P = 0.001$ (see online Supplemental Fig. 1).

Discussion

High-resolution DNA melting was first introduced in 2003 *(1, 18)*. It was rapidly adapted into most real-time

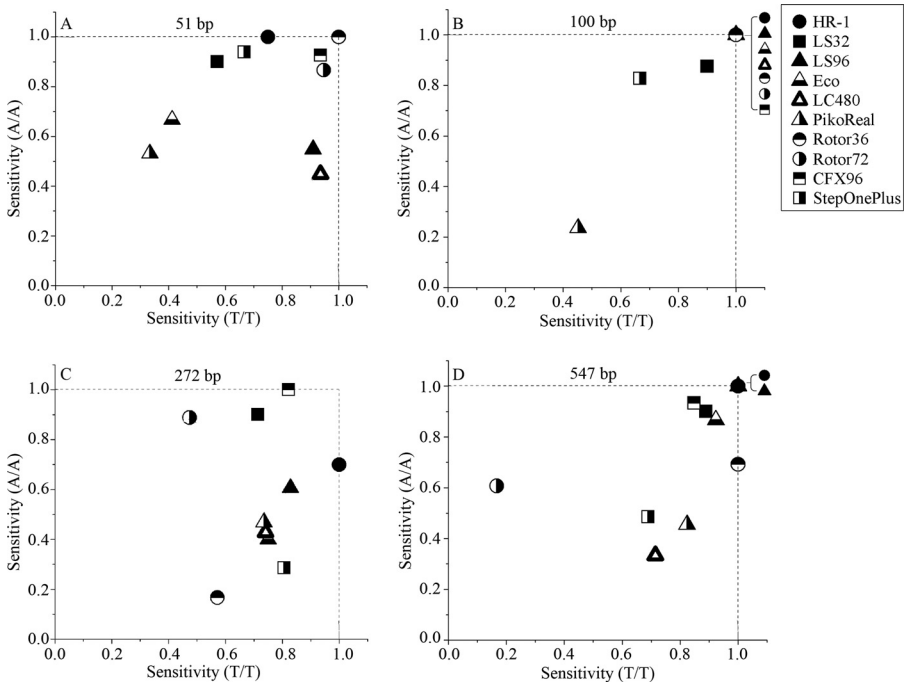

Fig. 3. Analytical sensitivity of homozygote detection across 10 instrument configurations and 4 PCR product sizes.
By plotting the sensitivity of detecting the T/T genotype against the A/A genotype, each panel correlates genotype sensitivities in 2 dimensions. Instruments with 100% accuracy appear at the top right corner. All samples were melted under manufacturers' recommended conditions and analyzed with the same custom software.

PCR instruments, often by slowing the melting rate down to obtain adequate resolution. The term "HRM" was trademarked by 1 instrument manufacturer, but there is no definition or standardization of what constitutes high-resolution melting, and recommended protocols vary widely among manufacturers. No guidelines such as Minimum Information for Publication of Quantitative Real-Time PCR Experiments *(21)* for quantitative PCR are available for melting.

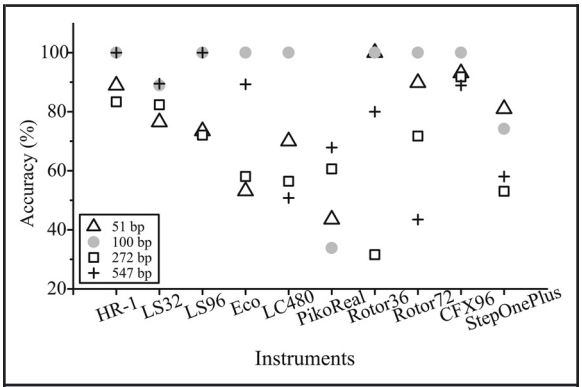

Fig. 4. Accuracy of homozygous genotyping on 10 instrument configurations with 4 PCR product lengths.
The instrument melting rates decrease from left to right as given in Table 1. The manufacturers' recommended melting conditions were used with custom analysis software.

Prior studies to establish instrument precision attempted to use constant melting rates of 0.1 °C/s, but in more than half the instruments, slower rates had to be used *(16)*. In this study, we focused on measuring the genotype accuracy of 10 different instrument configurations under the manufacturers' recommended conditions (ramp rates, sample volumes, number of samples, etc.), holding as many assay parameters constant as possible. We found that detection mode, analysis software, and PCR product size were highly significant factors that affected the genotyping accuracy of homozygotes.

The detection mode of an instrument refers to whether an instrument detects samples 1 at a time or by imaging multiple samples on a plate. Single sample detection can arise from only measuring 1 sample, or more commonly by scanning the optics over samples 1 at a time. Although imaging is convenient, single sample detection appears superior for differentiating ho-

mozygotes. Both fluorescence and temperature homogeneity can be compromised by spatial imaging, which adversely affects the precision of melting curves.

Use of a common software improved homozygote genotyping over manufacturers' software. This may result from the ability of the overlay function to focus on curve shape rather than position (T_m). This is surprising because homozygotes are usually differentiated by T_m, and curve overlay is not applied for fear of eliminating the major difference. However, our evidence suggests that curve overlay and shape differences can be used, at least in some cases, to better genotype homozygotes.

Early studies on PCR product length showed that the best accuracy for heterozygote detection occurred when PCR products were <400 bp *(10)*. Homozygous variant accuracy was assumed to depend on ΔT_m values that are greater with shorter PCR products *(18)*. Indeed, genotyping by high-resolution melting is often called "small amplicon genotyping." Our current data indicate that homozygote accuracy does depend on PCR product length, but the dependence is not a simple monotonic function. As the product length increases, the accuracy first goes up, then down, and finally up again. Although a general correlation with PCR product size and accuracy may exist, this appears to be highly sequence dependent. Better homozygote accuracy with multiple domains (as seen in the 547-bp product) has been suggested before *(5)* and may explain its improved accuracy over the 272-bp product.

The T_mSD has been used before as an important metric to predict temperature precision in melting instruments *(14)*. Our data correlate T_mSD with the detection mode. The T_mSD in instruments with full-plate imaging is about twice that observed in instruments with single sample detection. In addition to instrument factors, assay factors are important for genotyping accuracy, specifically the ΔT_m between the 2 homozygous genotypes. However, ΔT_m and T_mSD do not explain a majority of the variance in genotyping accuracy (see online Supplemental Fig. 1).

Limitations of this study include both instrument and assay limitations. Only certain instruments were available for study, and only a single instrument of each type was assessed. Some instruments were excluded from study because their optics did not match the dye used, and selected instruments may vary in the degree of optical matching. To focus on the instruments, the assay chemistries were held as constant as possible. Only 1 dye and 1 buffer composition were evaluated. Only 1 SNV and 4 PCR product lengths were genotyped. Because of these limitations, generalizations to other conditions (e.g., instruments and dyes) are tenuous.

The template was obtained by nested PCR to eliminate any differences in concentration or contaminants and pooled before melting. This removed variation attributable to PCR and focused only on melting. As such, our protocol could be considered a best-case scenario, not to be expected in real-world performance. However, we chose the worst-case scenario in the SNV, where homozygotes are predicted to have identical melting curves. Our purpose was to focus on melting and obtain different accuracies on different instruments to determine characteristics that affect genotyping accuracy.

Detection of gene variants by high-resolution melting depends on subtle melting curve differences, including shape changes and melting temperature shifts *(22–24)*. Alternate methods can been used to increase the detection sensitivity of melting assays, such as decreasing the PCR product length *(10)*, calibration with an internal oligonucleotide duplex *(13)*, quantitative heteroduplex analysis after mixing with a known genotype *(25)*, or the use of unlabeled probes *(14, 15)* or snapback primers *(26, 27)*. Nevertheless, melting of PCR products has an inherent simplicity that is very attractive. We hope to continue improving the accuracy of this method by identifying and implementing critical parameters. High-resolution melting is not a static achievement, but a continuum. As instruments and methods get better, so will melting accuracy and performance.

Author Contributions: *All authors confirmed they have contributed to the intellectual content of this paper and have met the following 3 requirements: (a) significant contributions to the conception and design, acquisition of data, or analysis and interpretation of data; (b) drafting or revising the article for intellectual content; and (c) final approval of the published article.*

Authors' Disclosures or Potential Conflicts of Interest: *Upon manuscript submission, all authors completed the author disclosure form. Disclosures and/or potential conflicts of interest:*

Employment or Leadership: C.T. Wittwer, *Clinical Chemistry*, AACC.
Consultant or Advisory Role: None declared.
Stock Ownership: None declared.
Honoraria: None declared.
Research Funding: M. Li, the China Scholarship Fund; C.T. Wittwer, BioFire Diagnostics, Canon US Life Sciences.
Expert Testimony: None declared.
Patents: R.A. Palais, US 8068992 B2, US 8296074 B2; C.T. Wittwer, US 6174670.
Other Remuneration: L. Zhou, University of Xiamen.

Role of Sponsor: The funding organizations played no role in the design of study, choice of enrolled patients, review and interpretation of data, or preparation or approval of manuscript.

Acknowledgments: We thank Ying Wang for technical assistance and Jesse Montgomery for reviewing the manuscript.

References

1. Wittwer CT, Reed GH, Gundry CN, Vandersteen JG, Pryor RJ. High-resolution genotyping by amplicon melting analysis using LCGreen. Clin Chem 2003;49:853–60.
2. Liew M, Pryor R, Palais R, Meadows C, Erali M, Lyon E, Wittwer C. Genotyping of single-nucleotide polymorphisms by high-resolution melting of small amplicons. Clin Chem 2004;50:1156–64.
3. Wittwer CT. High-resolution DNA melting analysis: advancements and limitations. Hum Mutat 2009;30:857–9.
4. Vossen RH, Aten E, Roos A, den Dunnen JT. High-resolution melting analysis (HRMA): more than just sequence variant screening. Hum Mutat 2009;30:860–6.
5. Montgomery JL, Sanford LN, Wittwer CT. High-resolution DNA melting analysis in clinical research and diagnostics. Expert Rev Mol Diagn 2010;10:219–40.
6. Zhou L, Palais RA, Ye F, Chen J, Montgomery JL, Wittwer CT. Symmetric snapback primers for scanning and genotyping of the cystic fibrosis transmembrane conductance regulator gene. Clin Chem 2013;59:1052–61.
7. Li M, Liu L, Liu Z, Yue S, Zhou L, Zhang Q, Cheng S, Li RW, Smith PN, Lu S. The status of KRAS mutations in patients with non-small cell lung cancers from mainland China. Oncol Rep 2009;22:1013–20.
8. Li M, Zhang Q, Liu L, Liu Z, Zhou L, Wang Z, Yue S, Xiong H, Feng L, Lu S. The different clinical significance of EGFR mutations in exon 19 and 21 in non-small cell lung cancer patients of China. Neoplasma 2011;58:74–81.
9. Dobrowolski SF, Wittwer CT. High resolution melt profiling. In: Rapley R, Harbron S, eds. Molecular analysis and genome discovery. Hoboken, NJ: Wiley 2011:81–113.
10. Reed GH, Wittwer CT. Sensitivity and specificity of single-nucleotide polymorphism scanning by high-resolution melting analysis. Clin Chem 2004;50:1748–54.
11. Santa Lucia J Jr, Hicks D. The thermodynamics of DNA structural motifs. Annu Rev Biophys Biomol Struct 2004;33:415–40.
12. Montgomery J, Wittwer CT, Kent JO, Zhou L. Scanning the cystic fibrosis transmembrane conductance regulator gene using high-resolution DNA melting analysis. Clin Chem 2007;53:1891–8.
13. Gundry CN, Dobrowolski SF, Martin YR, Robbins TC, Nay LM, Boyd N, Coyne T, Wall MD, Wittwer CT, Teng DH. Base-pair neutral homozygotes can be discriminated by calibrated high-resolution melting of small amplicons. Nucleic Acids Res 2008;36:3401–8.
14. Herrmann MG, Durtschi JD, Bromley LK, Wittwer CT, Voelkerding KV. Amplicon DNA melting analysis for mutation scanning and genotyping: cross-platform comparison of instruments and dyes. Clin Chem 2006;52:494–503.
15. Herrmann MG, Durtschi JD, Bromley LK, Wittwer CT, Voelkerding KV. Instrument comparison for heterozygote scanning of single and double heterozygotes: a correction and extension of Herrmann et al., Clin Chem 2006;52:494-503. Clin Chem 2007;53:150–2.
16. Herrmann MG, Durtschi JD, Wittwer CT, Voelkerding KV. Expanded instrument comparison of amplicon DNA melting analysis for mutation scanning and genotyping. Clin Chem 2007;53:1544–8.
17. Sanford LN, Wittwer CT. Monitoring temperature with fluorescence during real-time PCR and melting analysis. Anal Biochem 2013;434:26–33.
18. Gundry CN, Vandersteen JG, Reed GH, Pryor RJ, Chen J, Wittwer CT. Amplicon melting analysis with labeled primers: a closed-tube method for differentiating homozygotes and heterozygotes. Clin Chem 2003;49:396–406.
19. Palais R, Wittwer CT. Mathematical algorithms for high-resolution DNA melting analysis. Methods Enzymol 2009;454:323–43.
20. Dwight Z, Palais R, Wittwer CT. uMELT: prediction of high-resolution melting curves and dynamic melting profiles of PCR products in a rich web application. Bioinformatics 2011;27:1019–20.
21. Bustin SA, Benes V, Garson JA, Hellemans J, Huggett J, Kubista M, et al. The MIQE guidelines: minimum information for publication of quantitative real-time PCR experiments. Clin Chem 2009;55:611–22.
22. Vandersteen JG, Bayrak-Toydemir P, Palais RA, Wittwer CT. Identifying common genetic variants by high-resolution melting. Clin Chem 2007;53:1191–8.
23. Reed GH, Kent JO, Wittwer CT. High-resolution DNA melting analysis for simple and efficient molecular diagnostics. Pharmacogenomics 2007;8:597–608.
24. Erali M, Voelkerding KV, Wittwer CT. High resolution melting applications for clinical laboratory medicine. Exp Mol Pathol 2008;85:50–8.
25. Palais RA, Liew MA, Wittwer CT. Quantitative heteroduplex analysis for single nucleotide polymorphism genotyping. Anal Biochem 2005;346:167–75.
26. Zhou L, Errigo RJ, Lu H, Poritz MA, Seipp MT, Wittwer CT. Snapback primer genotyping with saturating DNA dye and melting analysis. Clin Chem 2008;54:1648–56.
27. Farrar JS, Palais RA, Wittwer CT. Snapback primer genotyping of the Gilbert syndrome UGT1A1 (TA)(n) promoter polymorphism by high-resolution melting. Clin Chem 2011;57:1303–10.